



Prediction of new MAX phase Zr_2MSiC_2 ($M = Ti, V$) compounds as a promising candidate for future engineering: DFT calculations

D. Behera^a, Aparna Dixit^b, Ahmed Azzouz-Rached^c, Ali Bentouaf^d, Md. Ferdous Rahman^e, Hind Albalawi^f, Abdessalem Bouhenna^g, El Sayed Yousef^{h,i}, Ramesh Sharma^{j,*}

^a Dept. of Physics, Birla Institute of Technology, Mesra, Jharkhand 835215, India

^b Department Basic Science and Humanities, Pranveer Singh Institute of Technology, Kanpur-209305, U.P., India

^c Magnetic Materials Laboratory, Faculty of Exact Sciences, Djillali Liabes University of Sidi Bel-Abbes, 22000 Sidi Bel-Abbes, Algeria

^d Faculty of Technology, Dr. Moulay, Tahar University of Saida, 20000 Saida, Algeria

^e Advanced Energy Materials and Solar Cell Research Laboratory, Department of Electrical and Electronic Engineering, Begum Rokeya University, Rangpur 5400, Bangladesh

^f Department of Physics, College of Sciences, Princess Nourah bint Abdulrahman University (PNU), P.O. Box 84428, Riyadh 11671, Saudi Arabia

^g Department of Physics, Faculty of Exact Sciences and Informatics, Hassiba Benbouali University of Chlef, Algeria

^h Research Centre for Advanced Materials Science (RCAMS), King Khalid University, Abha 61413, P.O. Box 9004, Saudi Arabia

ⁱ Physics Department, Faculty of Science, King Khalid University, P. O. Box 9004, Abha, Saudi Arabia

^j Department of Applied Science, Feroze Gandhi Institute of Engineering and Technology, Raebereli 229001, Uttar Pradesh, India

ARTICLE INFO

Keywords:

MAX phase
First principle method
Structural properties
Vicker hardness
Thermal properties

ABSTRACT

The Wien2K code, which utilizes density functional theory (DFT) first-principles method, is employed to examine the physical features of MAX phase Zr_2MSiC_2 ($M = Ti$ or V). Furthermore, this method is also used to determine the Debye temperature and Vickers hardness of the compound. The computed structural parameters are highly realistic. Calculation of the formation energy, elastic constants C_{ij} , and phonon band structure has confirmed with certainty compounds are thermodynamically, and mechanically stable. On the other hand, both Poisson's and Pugh's ratios reveal the compound's brittleness. The substance exhibits considerable elastic anisotropy. According to the electronic structure, our compounds contain a combination of ionic and metallic bonding. The melting temperature, Debye temperature, and minimum thermal conductivity confirm their use in harsh environments and as thermal barrier coatings. The fact that the rate of increase in Cv and the thermal expansion coefficient is the same in both compounds under varying pressure and temperature conditions suggests that they possess similar properties. The results that are being reported here increase the possible application of Zr_2MSiC_2 for future engineering.

1. Introduction

Metallic materials often exhibit properties such as thermal and electrical conductivity, plastic deformability at room temperature, ease of machining, resistance to thermal shock, damage tolerance, and relative softness. On the other hand, ceramics typically exhibit high elastic moduli, superior elastic features and resistance to corrosion, etc[1–4]. Materials with a desirable combination of both metallic and ceramic properties have been made possible by the relatively recent discovery of a class of novel materials called the MAX phases, sometimes known as “metallic ceramics.” A collection of carbides, nitrides, and borides constitute the MAX phases with the empirical formula $Mn_{+1}AX_n$, where

n corresponds to integers, early transition metals are M , from groups (13) to (16), and X is either C/B. They crystallize to hexagonal $P6_3/mc$ structure[5–8]. Around half of the MAX phase, $n = 1$ referred to as “H-phases” by Nowotny et al. in the 1960s[9]. However, for two decades, they were mostly disregarded, but by outlining outstanding characteristics of Ti_3SiC_2 , demonstrating that the other MAX phases shared these characteristics, and finally creating the word and definition currently used to refer to a “MAX phase,” Barsoum and El-Raghy rekindled interest in them in 1996, proving that the other MAX phases shared the same traits, and ultimately coming up with the term and definition that are now used to refer to a “MAX phase”[2,10–12]. Because of the way they are built by stacking n “ceramic” layers of MX between an A “metallic”

* Corresponding author.

E-mail address: sharmadft@gmail.com (R. Sharma).

plane, MAX phases have both ceramic and metallic characteristics (large thermal shock resistance, optimum mechanical stability, outstanding electrical conductivity etc. The MAX phases have both ceramic as well as metallic attributes, involving substantial resilience at elevated temperatures, capacity to resist oxidation as well as thermal shock, beneficial destruction tolerance and electrical conductivity[13]. This is because of the MAX phases' anisotropic hexagonal structure. Because of these difficult characteristics, MAX phases are widely used in spintronics, nuclear sector superconducting materials, and Li-ion batteries. Researchers recently enhanced the versatility and efficiency of MAX phase materials in compliance with demands. The results of this research could range from the identification of novel MAX phases to the blending of already known phases. Studies have also been conducted to determine the impact of atom incorporation and point defects on the characteristics of MAX phases. They exhibit the transition from brittle to ductile at extremely high temperatures. Exploring different stable bulk MAX phases for $n = 1\text{--}3$ has been challenging since the middle of the 2000s, suggesting that the true attainable list is nearly complete[14–16]. Again, apart from standard MAX phases, a number of derivative MAX phases, including $\text{Ti}_5\text{Al}_2\text{C}_3$, $\text{Ti}_5\text{Si}_2\text{C}_3$, have been observed. 24 MAX phase compounds, a few of which also appeared with different n values and of which at least one component has already been published, were recently described by Naguib et al[17]. Additionally, $\text{Ti}_2\text{Al}(\text{C}_{0.5}\text{N}_{0.5})$ as well as its derivative compounds has already reported for the Ti-Al systems having both C and N atoms[18,19]. However, the more studies have been reported in recent years due to their interesting mechanical as well as physical properties demanding materials with a wide range of possible engineering applications. Recently reported materials include $\text{Mo}_2\text{Ga}_2\text{C}$, $\text{Ti}_2\text{Au}_2\text{C}$, and $\text{Ti}_3\text{Au}_2\text{C}_2$ having twice A layer phases[3]. The reported materials have inspired the development of novel MAX phases and like compounds, which are continuously being defined. A thorough list of all known MAX phases was just recently published by Sokol et al. increasing the total to 155[20]. The MAX phase compounds Mn_2GaC , Zr_2AlC , as well as V_4AlC_3 are a few noteworthy contributions. Hu et al. found the V_4AlC_3 , which, to our knowledge, is the first and considered to be single 413-type MAX phase containing V[21]. Whereas other V-based MAX phases are reported with 211-type. Few investigations have been done on the V-Sn-C type. Recent research has produced a small number of multi-element with magnetic properties of A layers with formulation $\text{V}_2(\text{AxSn}_{1-x}\text{C}$ ($\text{A} = \text{Ni, Mn, or their arrangements}$)[21]. These phases exhibited ferromagnetic (FM) behavior as a result of the insertion of magnetic element at A having 211 types. Based on first-principles

calculations, have thoroughly examined 240 M2AX phases where the stability of V_2SnC was examined and it was discovered that this compound was inherently stable. However, there hasn't been any experimental proof of V_2SnC to date. Unknown are the crystal structure and the whole set of XRD data. Given that the constituent elements of MAX phases share a lot of chemical similarities and that other Sn-based MAX phases, like Ti_2SnC have excellent electrical conductivity[22], the MAX phase V_2SnC may one day be used as an electrical composite in the reinforcement of metals and polymers. Sn-containing MAX phases for the A element have drawn the greatest attention for two reasons: First, a recent study finds that Ti_2SnC exhibits effective mechanical damage recovery through fracture self-healing properties following the oxidation at low temperature. Recently, two novel $\text{Mo}_2\text{TiAlC}_2$ and $\text{Mo}_2\text{Ti}_2\text{AlC}_3$ solid solution MAX were found by Anasori et al[23]. They also established where the Mo and Ti atom layers in the crystal structure were located. A high purity, dense $\text{Mo}_2\text{Ti}_2\text{AlC}_3$ sample with a relative density of 99.3 % was also created by Fu et al. using the hot-pressing method, and its mechanical and physical features were in-depthly examined[24]. According to Fu et al., $\text{Mo}_2\text{Ti}_2\text{AlC}_3$ ceramic has the lowest thermal conductivity of any known MAX phases, measuring $6.82 \text{ W}(\text{mK})^{-1}$. However, experimental studies on the fundamental mechanical and physical characteristics of $\text{Mo}_2\text{TiAlC}_2$ were extremely scarce until the year 2020. Zr_2AlC is very significant, especially for the nuclear industry, due to its constituent components' maximum neutron transparency and possibility for providing reasonable radiation resistant performance, as seen in earlier MAX phases. This is in conjunction to $\text{Cr}_2\text{TiAlC}_2$ and $\text{V}_{1.5}\text{Cr}_{1.5}\text{AlC}_2$, which have already been discovered and reported, respectively, by Liu et al[25,26]. It should be noted that $\text{V}_{1.5}\text{Cr}_{1.5}\text{AlC}_2$ has a slightly organized structure. Dahlqvist et al. reported the stability of TiMAlC , TiM_2AlC_2 , and $\text{Ti}_2\text{M}_2\text{AlC}_3$, where M is from Periodic table group 4–6[27]. The studies by M. Bendjemai et al and I. Ouadha et al. on the MAX phases M_2ScSnC_2 , and Mn_2VSnC_2 , respectively, have shown that these compounds are both mechanically and dynamically stable[28]. Furthermore, their mechanical properties make them promising candidates for use in harsh environments such as thermal barrier coatings. Consequently, more information is needed to predict potential importance in a range of technological applications, including mechanical qualities, elastic anisotropic, Vickers hardness, thermal, and optical attributes. Vickers hardness, elastic anisotropy, and the study of mechanical properties all contribute to our understanding of how they could be used as structural elements or in other relevant contexts. Knowing something about thermal properties beforehand makes it simpler to distinguish compounds for the high temperature usage. Forecasting the possible uses of materials in coating technology can be done by looking into energy dependent mechanical parameters. Therefore, it is vital to investigate the aforementioned properties, which is what we have done in this study for the Zr_2MSiC_2 ($\text{M} = \text{Ti, V}$).

Table 1
The Wyckoff positions of the currently known polymorphs.

Atom	Site	coordinates			
α -polymorph					
	Wyckof	x	y	z	Z_i -range
$\text{M}_1(\text{Ti/V})$	4f	0	0	0
$\text{M}_{\text{II}}(\text{Zr})$	2a	1 $\frac{1}{3}$	2 $\frac{2}{3}$	Z_{M}	$0.1340827^1/0.131526^2$
A(Sn)	2d	0	0	$\frac{1}{4}$
X(C)	4f	2 $\frac{2}{3}$	1 $\frac{1}{3}$	Z_{C}	$0.067425^1/0.062880^2$
β -polymorph					
	Wyckof	x	y	z	Z_i -range
$\text{M}_1(\text{Ti})$	4f	0	0	0
$\text{M}_{\text{II}}(\text{Zr})$	2a	1 $\frac{1}{3}$	2 $\frac{2}{3}$	Z_{M}	$0.123024^1/0.123023^2$
A(Sn)	2d	1 $\frac{1}{3}$	2 $\frac{2}{3}$	$\frac{1}{4}$
X(C)	4f	2 $\frac{2}{3}$	1 $\frac{1}{3}$	Z_{C}	$0.072291^1/0.072291^2$

¹ $\text{Zr}_2\text{TiSiC}_2$.

² Zr_2VSiC_2 .

2. Computational methodology

The Wien2k code[29] and the linearized augmented plane wave approach(FP-LAPW)[30], part of DFT theory [31], are used to analyze the physical characteristics of Zr_2MSiC_2 . The PBE-GGA function has been considered as exchange–correlation [32]. The energy cutoff was set to -8 Ry and the Gmax is considered 12 in the present computation. For the Zr, V, Ti, V, Si, and C atoms, respectively, the muffin tin radius (Rmt) is 1.85, 1.99, 2.50, 2.29, 1.87 and 1.51 m (Bohr). In this computation, Kmax is equal to 8, which is the size of the biggest reciprocal vector module inside the Brillouin zone. We have listed structural details for 300 k-points in the Brillouin zone[33]. The formation energy (E_f , eV/atom) and estimated lattice constants of the optimized structure are mainly compared to experimental results. Zr_2MSiC_2 properties were calculated using the best-produced data by XC. A Monkhorst-Pack grid with dimensions of $12 \times 12 \times 12$ (k-points) was used to simulate the irreducible Brillouin zone. The criteria were set at 10^4 e/Bohr^3 and fewer than 10^5 Ry , respectively, for the energy and charge converging

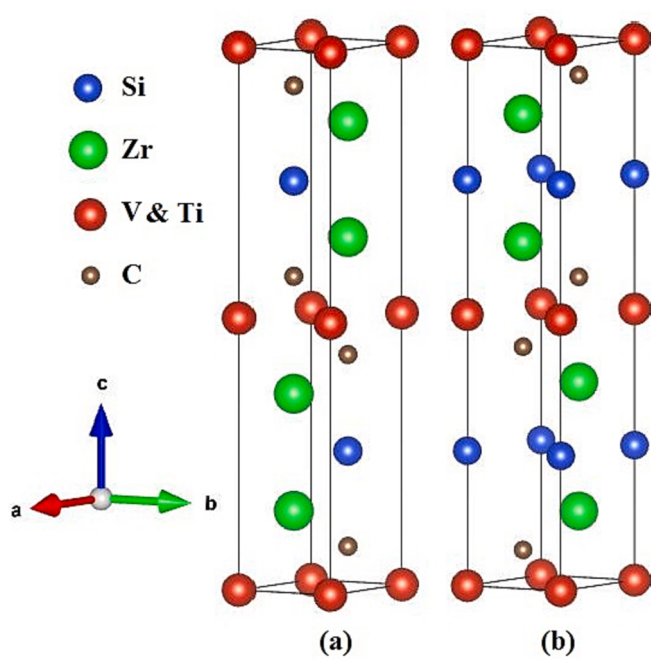


Fig. 1. A view of the crystal structure of the MAX phases $Zr_2M'SiC_2$: (a) α -polymorph (b) β -polymorph.

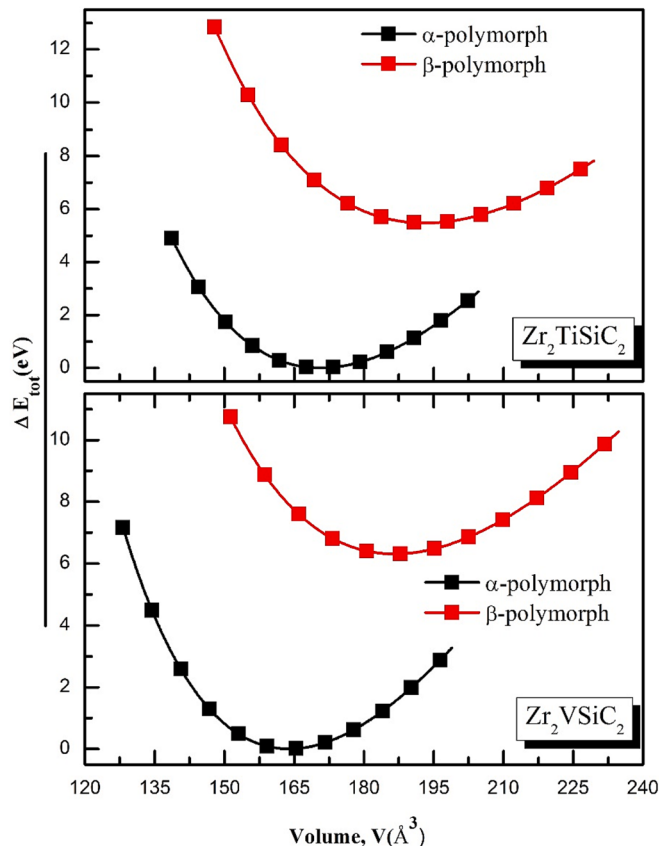


Fig. 2. Variation of the energy as a function of the volume for the (a) Zr_2TiSiC_2 and (b) Zr_2VSiC_2 .

self-consistent repetitions[34]. The second-order elastic constants (c_{ij}) were obtained by linearly fitting the estimated stress as a measure of strain. From the c_{ij} , the polycrystalline bulk modulus (B) and shear

modulus (G) were calculated using the Voigt, Reuss, and Hill approximations[35]. Using force constant matrices generated by the VASP implementation[36,37] of density functional perturbation theory (DFPT), the phonon band structure was determined. For a supercell of 32 atoms and an $8 \times 8 \times 4$ k-mesh, there was enough convergence concerning the forces.

3. Results and discussion

In this paper, we report on the ground-state features of the Zr_2MSiC_2 compounds as well as their thermodynamic and dynamic stability. In order to better understand these compounds' possible applications, our study also explores the physical, thermodynamic, and elastic properties of these substances. This is, as far as we are aware, the first publication on these Zr_2MSiC_2 compound characteristics.

3.1. Structural features

Zr_2MSiC_2 MAX phases are noticed to be in a hexagonal structure, with $P6_3/mmc$ (No. 194) space group. The Wyckoff locations of Zr_2MSiC_2 ($M = Ti,V$), are summarized in Table 1. The unit cell of Zr_2MSiC_2 compounds typically has twelve atoms, as seen in Fig. 1. Any ab-initio calculation starts by determining the crystalline structure's stable geometry and ideal orientation[13,17]. For each of the structures that were the focus of this work, the internal variable, the c/a proportion, and the (a, c) -parameter were all relaxed. The equilibrium cell volume was determined by modifying the cell morphology appropriate to various volumes using the conjugate gradient total energy minimization approach. To determine the ground state features that include the lattice parameter, energy, and bulk modulus the Birch-Murnaghan equation of state (EOS)[38] was matched to the collected data of energy against volume for each structure as shown in Fig. 2. It is observed that the α -polymorph has lowest energy as compared to others reflecting the stable crystal structure. The physical parameters associated with the polymorph are described in Table 2. These data have allowed us to determine that our results strongly concur with earlier ones[8,13]. The formation energy, however, is the most reliable indicator of a compound's stability. Due to the negative formation enthalpy values shown in Table 2 and the fact that Zr_2MSiC_2 ($M = Ti,V$) are thermodynamically stable, it should be viable to synthesize the phases under consideration. Additionally, greater stability typically results from higher negative formation enthalpy[39].

In order to verify the dynamical stability of Zr_2MSiC_2 ($M = Ti,V$), the phonon frequencies and phonon dispersion curves are computed using the linear response method and the supercell methodology. Fig. 3. displays resulting phonon dispersion curves. This is demonstrated by the lack of imaginary frequencies in the positive phonon dispersion curves (i.e., absence of negative dispersion curves) presented in Fig. 3.

3.2. Mechanical properties

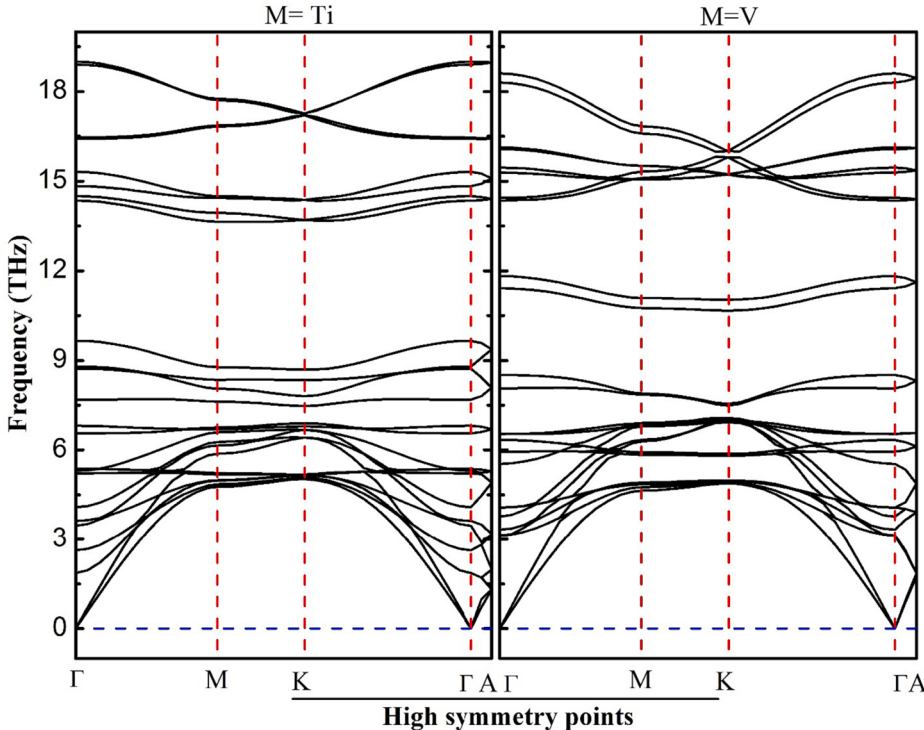
Materials' elastic constants affect how they behave mechanically. Since the elastic qualities of materials are linked to bonding features, the insight of elastic parameters corresponds to the chemical bonds that keep each atom of the substance intact. Zr_2MSiC_2 ($M = Ti,V$) is one of the MAX compounds, and its crystal geometry is hexagonal. As a result, six distinct elastic constants are acquired: C_{11} , C_{12} , C_{13} , C_{33} , C_{44} , and C_{66} etc [10,39]. The first five variables are considered to be independent considering the fact $C_{66} = (C_{11} - C_{12})/2$. It must meet the following conditions in order to be dynamically stable

$$\begin{cases} C_{11} > |C_{12}|, 2C_{13}^2 < C_{33}(C_{11} + C_{12}) \\ C_{44} > 0, C_{66} > 0 \end{cases} \quad (1)$$

The information related to the stiffness is approximated about the (100)

Table 2Computed lattice parameters, c/a ratio, bulk modulus (B), pressure derivative of the bulk modulus (B') and internal parameter [z (M) and z (X)].

Compounds	Phase	a (Å)	c (Å)	c/a	B (GPa)	B'	Energy (eV)	E_{form} (eV/atom)
$\text{Zr}_2\text{TiSiC}_2$	Our work	Alpha	3.26	18.52	5.68	184.68	4.01	-4.581668×10^5
		Beta	3.28	20.70	6.30	144.80	3.91	-4.581613×10^5
Zr_2VSiC_2	Our work	Alpha	3.21	18.30	5.69	194.11	4.13	-4.633625×10^5
		Beta	3.25	20.29	6.22	149.47	3.96	-4.405607×10^5

**Fig. 3.** Computed phonon dispersion for (a) $\text{Zr}_2\text{TiSiC}_2$ and (b) Zr_2VSiC_2 .

strain applying the C_{11} variable. Hence, $\text{Zr}_2\text{TiSiC}_2$ is regarded to be stiff as compared to the others under investigation. On the contrary, Zr_2VSiC_2 is the least rigid material [40]. The C_{12} , elastic constant measures the material's deformation in the (1 1 0). $\text{Zr}_2\text{TiSiC}_2$ is therefore the material that can be deformed the most readily[41]. Subject to the applied force on a- axis, $\text{Zr}_2\text{TiSiC}_2$ are quicker to fracture to other axes compared to Zr_2VSiC_2 as evidenced by the computed magnitude of C_{12} , C_{13} , as in **Table 2**. Last, but not least, it is found that Zr_2VSiC_2 has a smaller value of C_{33} than others, which makes it more quickly deformed via (0 0 1) compression under uniaxial stress.

The physical characteristics of these materials that depend on demonstrating their bearing strength include macroscopic mechanical properties. Additionally, it plays a crucial role in production engineering, as evidenced by the relevance of terms like Bulk as well as Shear Modulus (B and G), calculated using the Voigt Hill Reuss method and is expressed in the terms of the Voigt's approximation:

$$B_V = \frac{1}{2} (2(C_{11} + C_{12}) + 4C_{13} + C_{33}) \quad (2)$$

$$G_V = \frac{1}{30} (C_{11} + C_{12} + 2C_{33} - 4C_{13} + 12C_{55} + C_{66}) \quad (3)$$

Reuss's approximation

$$B_R = \frac{(C_{11} + C_{12})C_{33} - 2C_{13}^2}{C_{11} + C_{12} + 2C_{33} - 4C_{13}} \quad (4)$$

Table 3Computed elastic constants (C_{ij}) (in GPa).

Compound		C_{11}	C_{33}	C_{12}	C_{13}	C_{55}	C_{66}
$\text{Zr}_2\text{TiSiC}_2$	Our work	333	358	89	113	157	121
Zr_2VSiC_2	Our work	321	342	101	133	150	110

$$G_R = \frac{5}{20} \times \frac{C_{55}C_{66}[(C_{11} + C_{12})C_{33} - 2C_{13}^2]}{3B_V C_{44} C_{66} + \{(C_{11} + C_{12})C_{33} - 2C_{13}^2\}(C_{55} + C_{66})} \quad (5)$$

Hill's approximation

$$B_H = \frac{(B_V + B_R)}{2} \quad (6)$$

$$G_H = \frac{(G_V + G_R)}{2} \quad (7)$$

Furthermore, Young's modulus E along with Poisson's ratio ν are crucial mechanical constants and are expressed as

$$E = \frac{9BG}{(3B + G)} \quad (8)$$

$$\nu = \frac{(3B - 2G)}{2(3B + G)} \quad (9)$$

Table 3 displays the calculated values for the B, E, and G with an

Table 4

Computed elastic modulus (B, G and E) (in GPa), Poisson's ratio(v), G/B, Vickers hardness (H_V) (in GPa) and Cauchy pressure for two different directions for our compounds.

Compounds	B	G	B/G	E	H_V	v	P_X^{Cauchy}	P_Z^{Cauchy}
Zr ₂ TiSiC ₂	Our work	183	133	1.37	321	21	0.208	-43
Zr ₂ VSiC ₂	Our work	190	12	15.83	300	16	0.237	-17

emphasis on the bulk elastic parameters. Zr₂TiSiC₂ has been observed to be the minimum magnitude of B the lowest value of B and, hence, the lowest compression resistance, as is obvious[42]. Again, the more magnitude in G reflects the resistance to the stress thus the Zr₂VSiC₂ can be considered to have more resistance. The Pugh ratio (B/G) helps determine the brittle and ductile character of the studied compounds [43,44]. According to mathematics, a substance is deemed ductile when its Pugh's modulus is higher than 1.75, which implies that when plastic deformation occurs, a crack forms gradually. In contrast, brittle materials have rapid crack propagation despite little applied stress. Table 3 shows that Zr₂VSiC₂ is ductile while Zr₂TiSiC₂ is brittle in nature.

Although the shear anisotropic factors, which may assess the anisotropy in the holding between atoms in different planes, are particularly important. A few physical processes that largely rely on an understanding of shear anisotropic variables are the evolution of plastic distortion in substance, micro-scale cracking in ceramics, etc. The following equations are used to derive anisotropic shear factors A1, A2, and A3 for MAX phases.

$$A_1 = \frac{(C_{11} + C_{12} + 2C_{33} - 4C_{13})}{6C_{55}} \quad (10)$$

$$A_2 = \frac{2C_{55}}{(C_{11} - C_{12})} \quad (11)$$

$$A_3 = A_1 \cdot A_2 = \frac{(C_{11} + C_{12} + 2C_{33} - 4C_{13})}{3(C_{11} - C_{12})} \quad (12)$$

It is well known that the anisotropy factor Ai reflects the extent of elastic anisotropy of the crystalline and that when Ai = 1, the compound is entirely isotropic. By applying pushing force (tangential force) to screw dislocations, a high Ai value can help speed up the cross-slip pinning procedure. As shown in Table 4, the computed Ai-values for Zr₂MSiC₂ (M = Ti,V) solid solutions are close to unity, showing the evolution of the elastic anisotropy isotropy.

The anisotropic factor is a crucial factor that determines whether the MAX phase is more deformable along the a- or c-axis represented as Kc/Ka which can be obtained from the estimated elastic constants as determined Kc/Ka = (C₁₁ + C₁₃ - 2C₁₃)/(C₁₃ - C₁₁)[45]. It is evident that for Zr₂TiSiC₂ to have the compression along the a-axis that has at most similar magnitude along the c-axis too suggesting similar compression. The Poisson's ratio (v) predicts the nature of force (central/non-central) as well as its ductile/brittle nature[46]. Poisson's ratios 0.25–0.50 suggest the presence of central forces other than his it is considered to be noncentral. Moreover, a solid is ductile if the Poisson's ratio is higher than 0.26 and brittle if it is below. The computed results show that the Zr₂MSiC₂ (M = Ti,V) are central-force and brittle. The above result obtained is furthermore supported by Cauchy pressure[47].

Through the following relationships, the Cauchy pressure which is expressed by two distinct orientations, has been examined to support prior discoveries regarding the forms of solid failure and the chemical bonding characteristics

$$P_X^{Cauchy} = C_{13} - C_{55} \quad (13)$$

$$P_Z^{Cauchy} = C_{12} - C_{66} \quad (14)$$

Both are found to be negative supporting the earlier reports.

The preceding makes it clear that most of our MAX phases behave in

Table 5

Computed shear anisotropic parameters for the three different shear planes (A_1 , A_2 and A_3) and $\frac{K_c}{K_a}$.

Compounds	A_1	A_2	A_3	K_c/K_a
Zr ₂ TiSiC ₂	Our work	0.72	1.28	0.93
Zr ₂ VSiC ₂	Our work	0.63	1.36	0.87

a way that is more pliable and amenable to influence than the equivalent MXenes, making them better suited for use as anodes in Li-ion batteries (LIBs).

Science and technology are both interested in the study of thermal characteristics at high temperatures and pressures. Important thermal parameters include the Debye temperature, melting temperature, minimum thermal conductivity, and lattice thermal conductivity of Zr₂MSiC₂ (M = Ti,V). The Debye temperature (θ_D) is typically used to express a material's physical characteristics, including thermal expansion, thermal conductivity, lattice vibrations, melting temperature, and specific heat. It is also related to the superconducting transition temperature and the electron-phonon coupling constant in the context of superconductors [57]. The average sound velocity proposed by Anderson can be used to compute the Debye temperature and is related to the elastic module as follows:

$$\theta_D = \frac{h}{k_B} \left(\frac{3nN_A\rho}{4\pi M} \right)^{1/3} v_m \quad (15)$$

Where h is Planck's constant, N_A indicates Avogadro's number, and n is the number of atoms. Furthermore, the average velocity can be expressed

$$v_m = \left[\frac{1}{3} \left(\frac{2}{v_t^3} + \frac{1}{v_l^3} \right) \right]^{-\frac{1}{3}} \quad (16)$$

The v_t and v_l correspond to the transverse as well as longitudinal sound velocities, which are expressed in terms of the B and G as

$$v_t = \sqrt{\frac{G}{\rho}} \quad (17)$$

$$v_l = \sqrt{\frac{3B + 4G}{3\rho}} \quad (18)$$

The above parameters for the investigated Zr₂MSiC₂ (M = Ti,V) compounds are listed in Table 5. Here we can observe that all these parameters show little variation in the magnitude as listed in Table 5. Furthermore, it is known that the lower is the Debye temperature the material is considered to be soft. In this context, Zr₂VSiC₂ is considered to be softer as compared to other compounds under investigation which may lead to different engineering applications.

We have also looked into the melting temperature (Tm) of solid solutions of Zr₂MSiC₂ (M = Ti,V) which is used to indicate the purity of both organic and inorganic compounds. According to an empirical formula based on elastic constants created for hexagonal crystal by Fine et al., the Tm has been calculated:

$$T_m = 354 + \frac{3}{2}(2C_{11} + C_{33}) \quad (19)$$

Table 6

Computed density, longitudinal, transverse, and average elastic wave velocity [ρ (in g/cm³), v_l , v_t , v_m (in m/s)], the Debye temperatures (θ_D in K), Melting temperature (T_m in K), and minimum and lattice thermal conductivity at 300 K (k_{\min} , k_{ph} in W/m-K).

Compounds		ρ (g/cm ³)	v_l	v_t	v_m	θ_D	T_m	k_{\min}	k_{ph}
Zr ₂ TiSiC ₂	Our work	5.4951	8108.53	4923.28	5439.94	668.44	1891.66	0.61	81.85
Zr ₂ VSiC ₂	Our work	5.7864	7806.69	4580.39	5077.75	632.48	1834.01	0.59	56.96

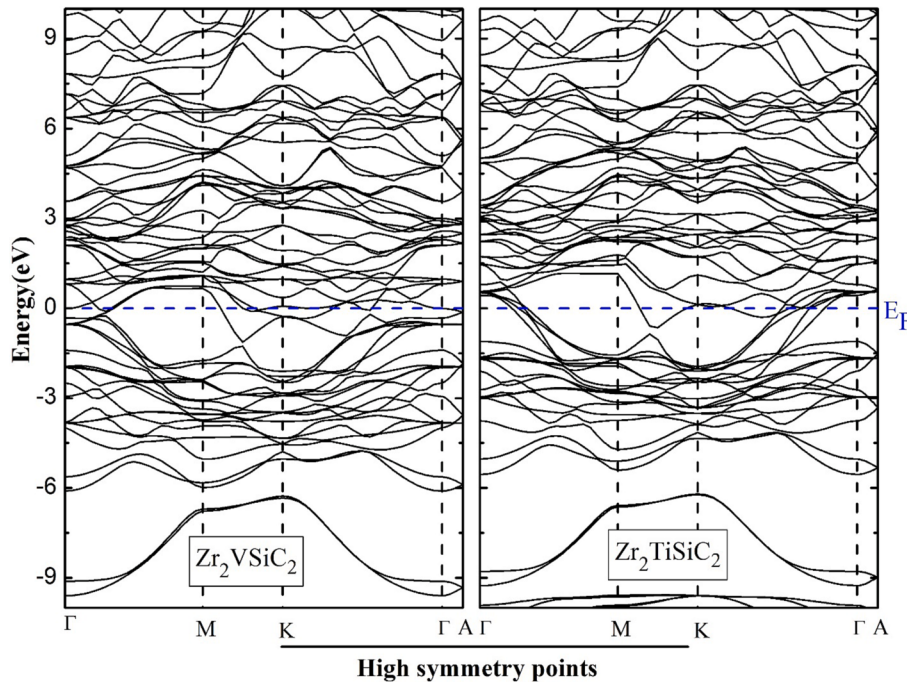


Fig. 4. Calculated the band structures for Zr₂M'SiC₂ along the high-symmetry axes of the first Brillouin zone.

Table 5 contains the predicted melting points for solid solutions of Zr₂MSiC₂ (M = Ti,V). The Tm is shown to decrease with increasing M concentrations. Tm is reduced by 5 % when Ti is completely replaced with V. The solid solutions Zr₂MSiC₂ (M = Ti,V) might potentially have applications in severe conditions because of their higher melting temperature.

One of the most crucial characteristics is the minimum thermal conductivity (k_{min}). The Clarke model is used to calculate min in the current stud:

$$\kappa_{\min} = k_B v_m \left(\frac{n N_A \rho}{M} \right) \quad (20)$$

Similar meanings are conveyed by the symbols used in this formulation as in Eq. (18). For Zr₂MSiC₂ (M = Ti,V), the predicted minimum thermal conductivity is stated in Table 6. It is evident that when M switches it drops. The minimum magnitude of it can conclude that the Zr₂MSiC₂ (M = Ti,V) shows it can be an ideal material for different manufacturing applications.

Slack et al. provided an equation to compute the lattice thermal conductivity (k_{ph}), taking into account the average atomic weight and the number of atoms in a “molecule” (or the atoms in the formula unit of the crystal)[48]. Due to their partially ceramic character, Slack’s model is appropriate to control the temperature-dependent k_{ph} of MAX phases, but Clarke’s model is highly helpful to determine the temperature-independent kind of compound. However, the empirical formula produced by Slack’s model can be used to determine the lattice thermal conductivity:

$$k_{ph} = A \frac{M_{av} \theta_D^3 \delta}{\gamma^2 n^{2/3} T} \quad (24)$$

In this equation, θ_D refers to the Debye temperature in K, n is the number of atoms in the unit cell, T is the temperature, and γ is the unites Grüneisen parameter[49]. This is obtained using the expression from the Poisson’s ratio:

$$\gamma = \frac{3(1 + \nu)}{2(2 - 3\nu)} \quad (25)$$

In addition, the factor $A(\gamma)$ due to Julian is calculated as:

$$A(\gamma) = \frac{5.720 \times 10^7 \times 0.849}{2 \times \left(1 - \frac{0.514}{\gamma} + \frac{0.228}{\gamma^2} \right)} \quad (26)$$

Table 5 lists the Zr₂MSiC₂ (M = Ti,V), k_{ph} determined at room temperature (300 K) the lower magnitude favors in different engineering applications.

3.3. Electronic properties

In this section, we investigate the electronic structure of the compounds to gain a deeper understanding of the operation of chemical bonding, electronic conductivity, electrical resistivity, and optical absorption. First, we calculated the band structure of the compounds that were the focus of this investigation along the higher symmetry points in the first Brillouin zone (BZ)[50]. The band structure results for the MAX phase compounds are shown in Fig. 4. As can be seen from these images, the band structure is topologically similar and displays a large amount of dispersion at the valence and conduction bands. A significant overlap between the valence and conduction bands at the Fermi level can also be found for the five compounds under consideration. This shows that the

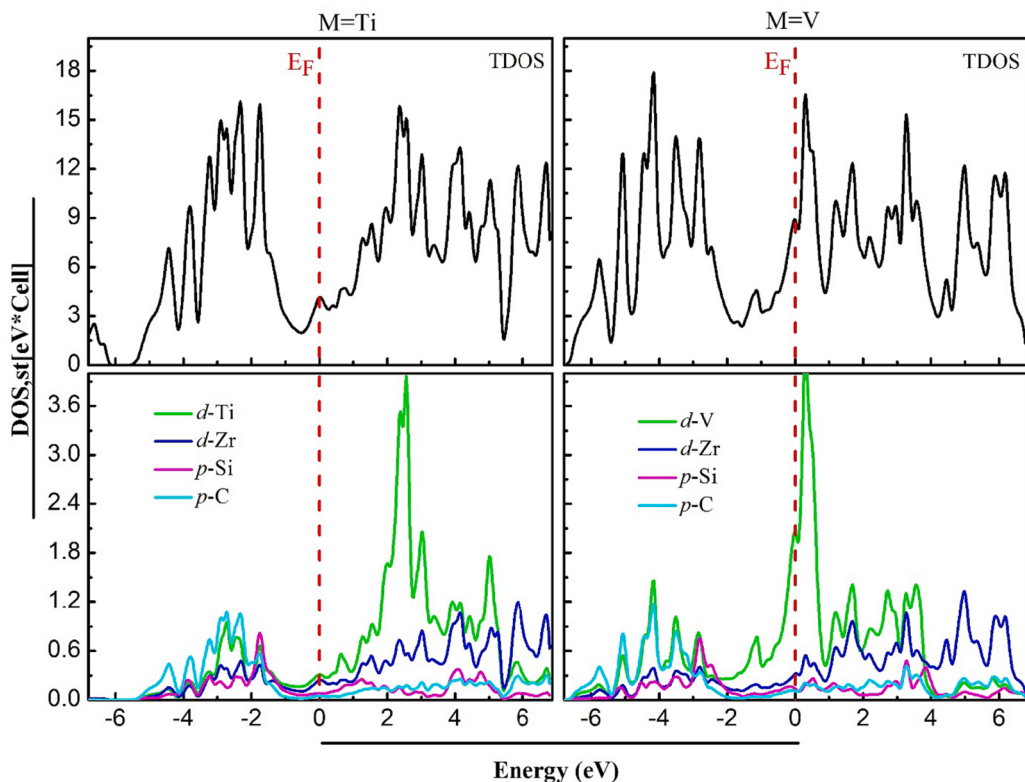


Fig. 5. Calculated Totals and Partials density of states (TDOS, PDOS) for (a) $\text{Zr}_2\text{TiSiC}_2$ and (b) Zr_2VSiC_2 .

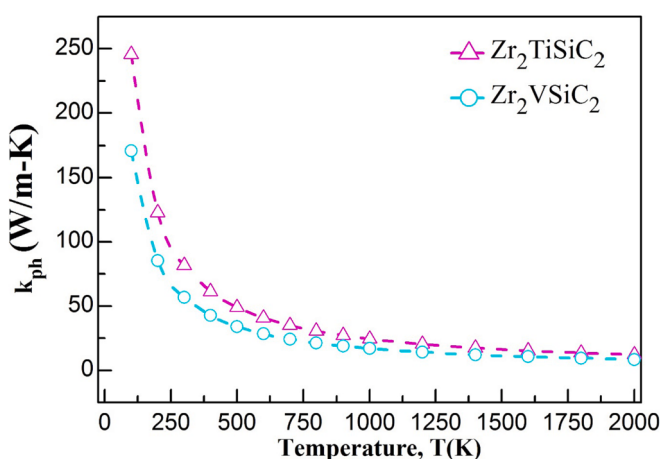


Fig. 6. Temperature dependence of lattice thermal conductivity.

substances are metallic. Second, the total density of states (TDOS) and projected density of states (PDOS) were examined over a wide energy range symmetric about the Fermi level. The TDOS and PDOS of Zr_2MSiC_2 ($M = \text{Ti}, \text{V}$), respectively, are shown in Fig. 5. The metallic nature of the compounds is supported by the TDOS's non-vanishing value at the Fermi level. Based on the PDOS data, we may further divide the DOS spectrum for the materials into three main zones. In the lower valence band region, it is possible to see the s-p hybridization between the p and d orbitals of the C and Ti/V atoms. The second location, which is near the Fermi level, has a substantial mixture of the d-(Zr) and p-C states, suggesting that there is a significant covalent bonding there. Our compounds' metallic properties are mostly a result of these potent covalent bonds. In the remaining region, there is less of a covalent bond between the d-Zr and p-C states. Collectively, these facts lend weight to the judgments made based on mechanical qualities.

3.4. Thermodynamic properties

The thermodynamic properties of Zr_2MSiC_2 ($M = \text{Ti}, \text{V}$) have been studied at high temperatures and pressures, including their lattice parameters, Debye temperature, heat capacity at constant volume, and the thermal expansion coefficient. In this study, we investigated the thermodynamic properties considering the quasi-harmonic Debye model using GiBBS2 package[51]. The k_{ph} values discovered at room temperature (300 K) are displayed in Fig. 6. Its dependence on temperature between 0 and 2000 K is illustrated, showing that as the temperature rises, the k_{ph} value falls. Zr_2MSiC_2 ($M = \text{Ti}, \text{V}$) have k_{ph} of 47.8 W/mk and 48.6 W/mk, respectively, at 300 K. The less k_{ph} magnitudes help in the usage of the investigated compounds in Max phase device applications. Fig. 7 represents the variation of Volume V as a function of temperature and pressure[52]. We may observe that as the temperature changes at particular pressures, the volume gradually increases. On the other hand, the volume has significantly decreased at a given temperature as pressure has increased. In ambient circumstances (0 GPa and 300 K), the volumes of Zr_2MSiC_2 ($M = \text{Ti}, \text{V}$) are determined to be 1065.32 Bohr³ and 1114.54 Bohr³, respectively. Fig. 8 depicts the temperature and pressure affect the evolution of the variation of specific heat at constant volume (C_v). The Petit Dulong limit[53,54] is approached C_v at high temperatures. The obtained values of the Dulong-Petit limit for Zr_2MSiC_2 ($M = \text{Ti}, \text{V}$) are 297.8 J.mol⁻¹ K⁻¹ and 296.9 J.mol⁻¹ K⁻¹, respectively. With the well-known Dulong and Petit's law $C_v \propto T^3$, the C_v rises quickly and becomes constant at high temperatures. We also notice that the temperature has a substantial effect on the C_v . Moreover, Fig. 9 illustrates the Debye temperature θ_D with temperature and pressure[55]. With a certain pressure, it can be shown that the θ_D progressively decreases up to 1000 K. It's interesting to note that θ_D becomes better as pressure increases from 0 to 30 GPa. For the compounds Zr_2MSiC_2 ($M = \text{Ti}, \text{V}$), the θ_D is calculated to be 580.2 K and 610.7 K, respectively, in the ambient conditions (0 GPa and 300 K). Fig. 10 depicts the variation of the coefficient of thermal expansion (α)

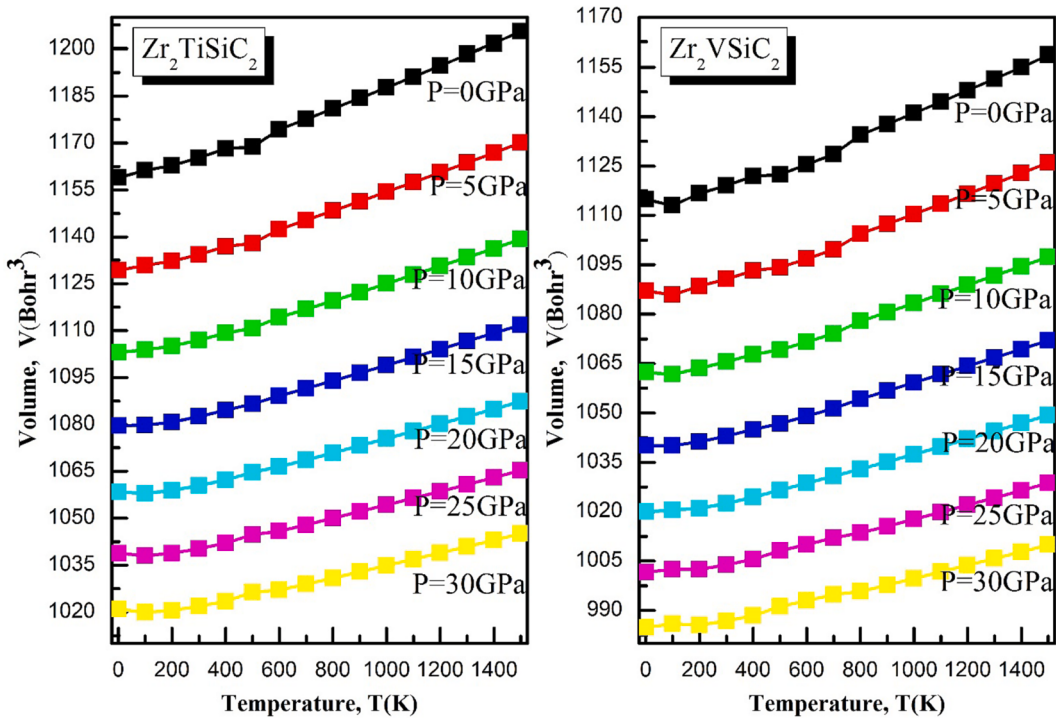


Fig. 7. The Volume (V) as a function of temperature at different pressure for the compounds $Zr_2M'SiC_2$.

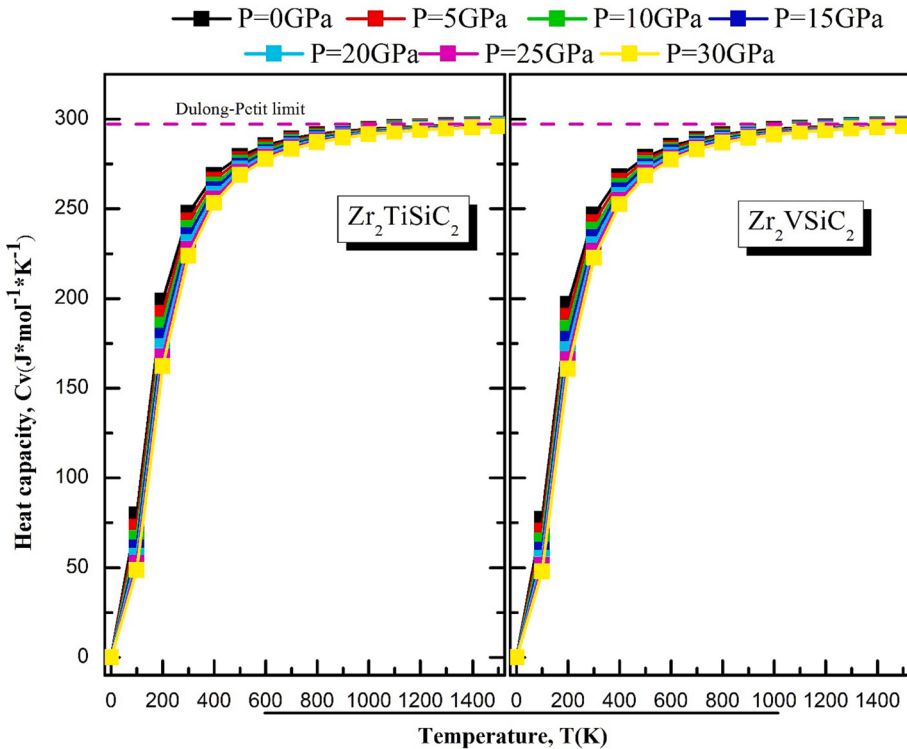


Fig. 8. The heat capacity (C_v) as a function of temperature at different pressure for the compounds $Zr_2M'SiC_2$.

with temperature and pressure. The graph shows that between 0 and 200 K, the temperature rises quickly, then gradually, and above 300 K, especially in high-pressure areas, the temperature rises virtually linearly with a low slope. The extensive analysis of the thermodynamic properties will provide insight into the experimental efforts.

4. Conclusions

The FP-LAPW method incorporated in the WIEN2k code was used to theoretically investigate the physical properties of two MAX phases, Zr_2TiSiC_2 and Zr_2VSiC_2 . Based on our findings, the results confirm that these compounds are thermodynamically, mechanically, and

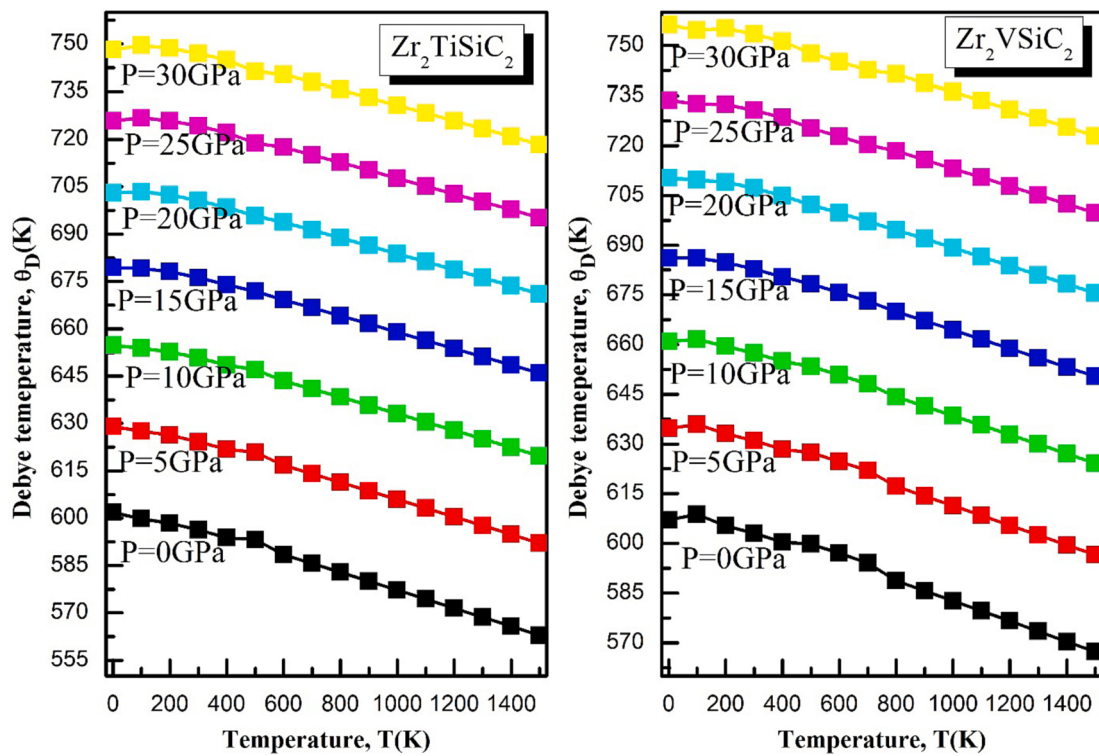


Fig. 9. Debye temperature (θ_D) as a function of temperature at different pressure for the compounds $Zr_2M'SiC_2$.

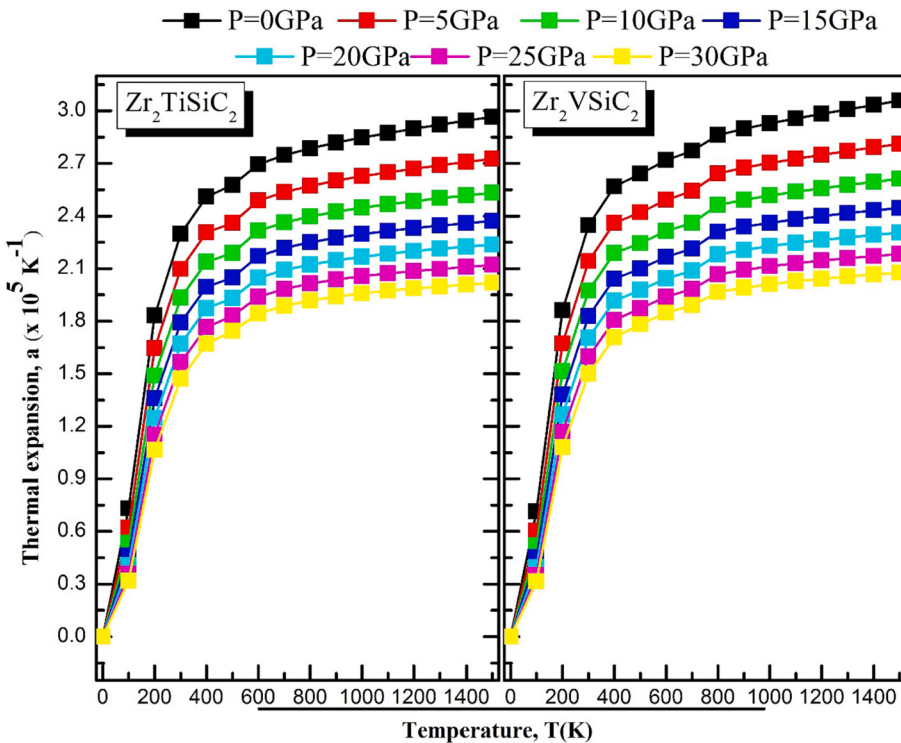


Fig. 10. Thermal expansion coefficient (α) as a function of temperature at different pressure for the compounds $Zr_2M'SiC_2$.

dynamically stable. We have determined that compounds Zr_2MSiC_2 exhibit brittle behavior and anisotropic characteristics as evidenced by Cauchy pressure, Pugh's ratio, and Poisson's ratio. Additionally, electronic structure calculations reveal ionic bonding and metallic properties for these compounds. Our estimations suggest that due to their high melting temperature and low minimum thermal conductivity, these

compounds have the potential for use in harsh environments and as thermal barrier coatings. As such, we hope that our study will inspire further experimental investigation into these materials by the MAX phase science community, to explore their potential for future applications.

CRediT authorship contribution statement

D. Behera: Writing – original draft. **Aparna Dixit:** Writing – review & editing. **Ahmed Azzouz-Rached:** Data curation. **Ali Bentouaf:** Formal analysis. **Md. Ferdous Rahman:** Supervision. **Hind Albalawi:** Writing – review & editing. **Abdessalem Bouhenna:** Methodology. **El Sayed Yousef:** . **Ramesh Sharma:** Writing – review & editing.

Declaration of Competing Interest

The authors declare that they have no known competing financial interests or personal relationships that could have appeared to influence the work reported in this paper.

Data availability

Data will be made available on request.

Acknowledgement

This research was funded by the Princess Nourah bint Abdulrahman University Researchers Supporting Project number (PNURSP2024R29), Princess Nourah bint Abdulrahman University, Riyadh, Saudi Arabia. The authors extend their appreciation to the Deanship of Scientific Research at King Khalid University for funding this work through research groups program under grant number (RGP.2/583/44).

Authorship statement

All persons who meet authorship criteria are listed as authors, and all authors certify that they have participated sufficiently in the work to take public responsibility for the content, including participation in the concept, design, analysis, writing, or revision of the manuscript.

References

- [1] M. Radovic, M.W. Barsoum, MAX phases: bridging the gap between metals and ceramics, *American Ceram. Soc. Bull.* 92 (2013) 20–27.
- [2] M.W. Barsoum, MAX phases: properties of machinable ternary carbides and nitrides, John Wiley & Sons, 2013.
- [3] M.A. Ali, M.M. Hossain, M.M. Uddin, A. Islam, D. Jana, S.H. Naqib, DFT insights into new B-containing 212 MAX phases: Hf2AB2 (A= In, Sn), *J. Alloy. Compd.* 860 (2021) 158408.
- [4] M. Naguib, V.N. Mochalin, M.W. Barsoum, Y. Gogotsi, 25th anniversary article: MXenes: a new family of two-dimensional materials, *Adv. Mater.* 26 (2014) 992–1005.
- [5] Z.M. Sun, Progress in research and development on MAX phases: a family of layered ternary compounds, *Int. Mater. Rev.* 56 (2011) 143–166.
- [6] C. Hu, F. Li, J. Zhang, J. Wang, J. Wang, Y. Zhou, Nb4AlC3: A new compound belonging to the MAX phases, *Scripta Comput. Sci. Appl. Math. Materialia.* 57 (2007) 893–896.
- [7] Y. Bai, N. Srikanth, C.K. Chua, K. Zhou, Density Functional Theory Study of Mn+1AXn Phases: A Review, *Crit. Rev. Solid State Mater. Sci.* 44 (2019) 56–107.
- [8] M.S. Hossain, M.A. Ali, M.M. Hossain, M.M. Uddin, Physical properties of predicted MAX phase borides Hf2AB (A= Pb, Bi): A DFT insight, *Mater. Today Commun.* 27 (2021) 102411.
- [9] W. Jeitschko, H.T. Nowotny, F. Benesovsky, Carbides of formula T2MC, *Journal of the Less Common Metals.* 7 (1964) 133–138.
- [10] M.W. Barsoum, M. Radovic, Elastic and mechanical properties of the MAX phases, *Annu. Rev. Mat. Res.* 41 (2011) 195–227.
- [11] M.A. Ali, M.M. Hossain, M.M. Uddin, M.A. Hossain, A. Islam, S.H. Naqib, Physical properties of new MAX phase borides M2SB (M= Zr, Hf and Nb) in comparison with conventional MAX phase carbides M2SC (M= Zr, Hf and Nb): Comprehensive insights, *J. Mater. Res. Technol.* 11 (2021) 1000–1018.
- [12] I. Ouadha, H. Rached, A. Azzouz-Rached, A. Reggad, D. Rached, Study of the structural, mechanical and thermodynamic properties of the new MAX phase compounds (Zr1-xTix) 3AlC2, *Comput. Condens. Matter.* 23 (2020) e00468.
- [13] A. Azzouz-Rached, H. Rached, M.H. Babu, T. Hadji, D. Rached, Prediction of double transition metal (Cr1-xZrx) 2AlC MAX phases as thermal barrier coatings: Insight from density functional theory, *Int. J. Quantum Chem.* 121 (2021) e26770.
- [14] Y. Mo, P. Rulis, W.Y. Ching, Electronic structure and optical conductivities of 20 MAX-phase compounds, *Phys. Rev. B* 86 (2012) 165122.
- [15] W. Ching, Y. Mo, S. Aryal, P. Rulis, Intrinsic mechanical properties of 20 MAX-phase compounds, *J. Am. Ceram. Soc.* 96 (2013) 2292–2297.
- [16] A. Azzouz-Rached, M.A. Hadi, H. Rached, T. Hadji, D. Rached, A. Bouhemadou, Pressure effects on the structural, elastic, magnetic and thermodynamic properties of Mn2AlC and Mn2SiC MAX phases, *J. Alloy. Compd.* 885 (2021) 160998.
- [17] M. Naguib, G.W. Bentzel, J. Shah, J. Halim, E.N. Caspi, J. Lu, L. Hultman, M.W. Barsoum, New Solid Solution MAX Phases:(TiO. 5, VO. 5) 3AlC2,(NbO. 5, VO. 5) 2AlC,(NbO. 5, VO. 5) 4AlC3 and (NbO. 8, ZrO. 2) 2AlC, *Mater. Res. Lett.* 2 (2014) 233–240.
- [18] V. Gray, Ti3SiC2 and Ti3AlC2 Single Crystal Elastic Shear Modulus: Investigation via Inelastic Neutron Scattering and Computer Simulation, (2013).
- [19] Z. Xiao, S. Ruan, L.B. Kong, W. Que, K. Zhou, Y. Liu, T. Zhang, MXenes and MXenes-based composites, Springer, 2020.
- [20] I.M. Chirica, A.G. Mirea, S. Neațu, M. Florea, M.W. Barsoum, F. Neațu, Applications of MAX phases and MXenes as catalysts, *J. Mater. Chem. A* 9 (2021) 19589–19612.
- [21] Q. Xu, Y. Zhou, H. Zhang, A. Jiang, Q. Tao, J. Lu, J. Rosén, Y. Niu, S. Grasso, C. Hu, Theoretical prediction, synthesis, and crystal structure determination of new MAX phase compound V 2 SnC, *J. Adv. Ceram.* 9 (2020) 481–492.
- [22] Q. Zhang, Z. Tian, P. Zhang, Y. Zhang, Y. Liu, W. He, L. Pan, Y. Liu, Z. Sun, Rapid and massive growth of tin whisker on mechanochemically decomposed Ti2SnC, *Mater. Today Commun.* 31 (2022) 103466.
- [23] B. Anasori, M. Dahlqvist, J. Halim, E.J. Moon, J. Lu, B.C. Hosler, E.N. Caspi, S. J. May, L. Hultman, P. Eklund, Experimental and theoretical characterization of ordered MAX phases Mo2TiAlC2 and Mo2Ti2AlC3, *J. Appl. Phys.* 118 (2015).
- [24] S. Fu, Y. Liu, H. Zhang, S. Grasso, C. Hu, Synthesis and characterization of high purity Mo2Ti2AlC3 ceramic, *J. Alloy. Compd.* 815 (2020) 152485.
- [25] A. Petruhins, Synthesis and characterization of magnetic nanolaminated carbides, Linköping University Electronic Press, 2018.
- [26] A. Azzouz-Rached, H. Rached, I. Ouadha, D. Rached, A. Reggad, The Vanadium-doping effect on physical properties of the Zr2AlC MAX phase compound, *Mater. Chem. Phys.* 260 (2021) 124189.
- [27] M. Dahlqvist, J. Rosen, Order and disorder in quaternary atomic laminates from first-principles calculations, *PCCP* 17 (2015) 31810–31821.
- [28] M. Bendjemai, A.A. Rached, M. Husain, A. Bentouaf, N. Rahman, V. Tirth, A. Algahtani, A.H. Alghatlani, T. Al-Mughanam, First-principles calculations to investigate structural, elastic and thermodynamic properties of new M2ScSnC2 (M= V or Nb) quaternary compounds for 312 MAX phases, *J. Mater. Res. Technol.* 24 (2023) 3211–3221.
- [29] P. Blaha, K. Schwarz, G. Madsen, D. Kvasnicka, J. Luitz, Inst. f. Materials Chemistry, TU Vienna, [Http://Www.Wien2k.At](http://Www.Wien2k.At) (n.d.).
- [30] P. Blaha, K. Schwarz, P. Sorantin, S.B. Trickey, Full-potential, linearized augmented plane wave programs for crystalline systems, *Comput. Phys. Commun.* 59 (1990) 399–415.
- [31] L.J. Sham, M. Schlüter, Density-functional theory of the energy gap, *Phys. Rev. Lett.* 51 (1983) 1888.
- [32] J.P. Perdew, K. Burke, M. Ernzerhof, Generalized gradient approximation made simple, *Phys. Rev. Lett.* 77 (1996) 3865.
- [33] D. Behera, A. Azzouz-Rached, A. Bouhenna, M.M. Salah, A. Shaker, S. K. Mukherjee, First-Principles Studies on the Physical Properties of the Half Heusler RbNbCd and RbNbZn Compounds: A Promising Material for Thermoelectric Applications, *Crystals* 13 (2023) 618.
- [34] M. Manzoor, D. Behera, S. Chowdhury, R. Sharma, M.W. Iqbal, S.K. Mukherjee, S. S. Alarfaji, H.A. Alzahrani, First-principles calculations to investigate structural, dynamical, thermodynamic and thermoelectric properties of CdYF3 perovskite, *Comput. Theor. Chem.* 1217 (2022) 113928.
- [35] L. Zuo, M. Humbert, C. Esling, Elastic properties of polycrystals in the Voigt-Reuss-Hill approximation, *J. Appl. Cryst.* 25 (1992) 751–755.
- [36] J. Hafner, Materials simulations using VASP—a quantum perspective to materials science, accessed December 1, 2021, *Comput. Phys. Commun.* 177 (2007) 6–13, https://www.sciencedirect.com/science/article/pii/S001046550700080X?casa_token=ZfGiGL5nbREAAAA:e1u-tDmyB4wHipdnRp8HHW6A5c9cVHwH3GleoeTRsNtp3NEsUJS06hH1FC5pS0YaaZvhq5sY.
- [37] J. Hafner, Ab-initio simulations of materials using VASP: Density-functional theory and beyond, *J. Comput. Chem.* 29 (2008) 2044–2078, <https://doi.org/10.1002/jcc.21057>.
- [38] T. Katsura, Y. Tange, A simple derivation of the Birch-Murnaghan equations of state (EOSs) and comparison with EOSs derived from other definitions of finite strain, *Minerals.* 9 (2019) 745.
- [39] D. Behera, S.K. Mukherjee, Structural, elastic, electronic and thermoelectric properties of K2GeBr6: A first principle approach, *Mater. Today: Proc.* (2023).
- [40] S. Lakra, S. Kumar Mukherjee, Study of structural, electronic, optical and thermodynamic properties of SnSiO3 compound: A DFT study, *Mater. Today: Proc.* (2023). 10.1016/j.mtpr.2023.01.231.
- [41] D. Behera, S.K. Mukherjee, Optoelectronics and Transport Phenomena in Rb2InBiX6 (X= Cl, Br) Compounds for Renewable Energy Applications: A DFT Insight, *Chemistry* 4 (2022) 1044–1059.
- [42] A.S. Verma, A. Kumar, Bulk modulus of cubic perovskites, *J. Alloy. Compd.* 541 (2012) 210–214.
- [43] S.F. Pugh, XCII. Relations between the elastic moduli and the plastic properties of polycrystalline pure metals, *London, Edinburgh, Dublin Philos. Magazine J. Sci.* 45 (1954) 823–843.
- [44] A. Azzouz-Rached, M.W. Qureshi, I. Ouadha, H. Rached, T. Hadji, H. Rekab-Djabri, DFT analysis of physical properties of quaternary MAX phase nitrides:(Fe0.5M0.5) 2SiN (M= Cr & Mn), *Comput. Condens. Matter.* 33 (2022) e00748.
- [45] G. Surucu, Investigation of structural, electronic, anisotropic elastic, and lattice dynamical properties of MAX phases borides: An Ab-initio study on hypothetical

- M2AB (M= Ti, Zr, Hf; A= Al, Ga, In) compounds, *Mater. Chem. Phys.* 203 (2018) 106–117.
- [46] A. Dixit, A. Saxena, D. Behera, J.A. Abraham, R. Sharma, S.K. Mukherjee, First principles study on structural, mechanical, and thermoelectric properties of half-Heusler alloy (KLiTe), *Mater. Today: Proc.* (2023).
- [47] M.E. Eberhart, T.E. Jones, Cauchy pressure and the generalized bonding model for nonmagnetic bcc transition metals, *Phys. Rev. B* 86 (2012) 134106.
- [48] G.A. Slack, Nonmetallic crystals with high thermal conductivity, *J. Phys. Chem. Solid* 34 (1973) 321–335.
- [49] Y.-Q. Zhao, C.-E. Hu, L. Liu, Y. Cheng, L.-C. Cai, First-Principles Investigations on Structural, Elastic, Dynamical, and Thermal Properties of Earth-Abundant Nitride Semiconductor CaZn₂N₂ under Pressure, *Zeitschrift Für Naturforschung a* 72 (2017) 39–49.
- [50] D. Behera, R. Sharma, H. Ullah, H.S. Waheed, S.K. Mukherjee, Electronic, optical, and thermoelectric investigations of Zintl phase AAg₂Se₂ (A= Sr, Ba) compounds: A first first-principles approach, *J. Solid State Chem.* 123259 (2022).
- [51] A. Otero-de-la-Roza, V. Luña, Gibbs2: A new version of the quasi-harmonic model code. I. Robust treatment of the static data, *Comput. Phys. Commun.* 182 (2011) 1708–1720.
- [52] D. Behera, A. Dixit, B. Nahak, A. Srivastava, S. Dubey, R. Sharma, A.K. Mishra, S. K. Mukherjee, Structural, electronic, elastic, vibrational and thermodynamic properties of antiperovskites Mg₃NX (X= Ge, Sn): A DFT study, *Phys. Lett. A* 453 (2022) 128478.
- [53] R.K. Fitzgerel, F.H. Verhoek, The law of Dulong and Petit, (1960).
- [54] E.I. Andritsos, E. Zarkadoula, A.E. Phillips, M.T. Dove, C.J. Walker, V.V. Brazhkin, K. Trachenko, The heat capacity of matter beyond the Dulong-Petit value, *J. Phys. Condens. Matter* 25 (2013) 235401.
- [55] H. Inaba, T. Yamamoto, Debye temperature of materials, *Netsu Sokutei*. 10 (1983) 132–145.